

周期载荷下电活性聚合物圆柱壳的动力响应*

王成敏¹ 任九生²

(1. 上海市应用数学与力学研究所, 上海 200072)

(2. 上海大学力学系, 上海市力学在能源工程中的应用重点实验室, 上海 200444)

摘要 基于非线性动力学理论研究了不可压电活性聚合物圆柱壳在内表面周期载荷作用下的运动与破坏等动力响应问题. 通过对所得描述圆柱壳内表面运动的非线性常微分方程的数值计算和动力学定性分析, 发现存在临界载荷和临界电压; 当周期载荷的平均载荷值小于临界载荷及外加电压小于临界电压时, 圆柱壳的运动随时间的演化是拟周期性的非线性振动. 反之, 圆柱壳将被破坏. 讨论了外加电场和载荷参数对临界值和圆柱壳运动特性的影响.

关键词 电活性聚合物, 非线性常微分方程, 拟周期振动, 临界载荷, 破坏

DOI: 10.6052/1672-6553-2015-063

引言

近年来电活性聚合物(EAP)材料以其具有大变形、高能量质量比、高效率 and 响应速度快等优点引起了国内外学者的广泛关注^[1-2]. 电活性聚合物材料在移动机器人、‘医疗器械’、光学仪器等众多领域显示了广阔的应用前景^[3]. Pelrine 等发现一种硅电活性聚合物具有良好的性质, 它的变形、提供的压力及反应速度都优于自然肌肉体, 并且它的能量密度远远超过其它致动器材料^[4].

随着研究的不断深入, 电活性聚合物的失效引起了人们的高度重视, Suo 等利用线性弹性应变能函数对机电稳定性进行分析^[5-6]. Plante 针对菱形、环形驱动器的失效行为进行了理论分析与试验研究, 分析了驱动器工作速度对其失效行为的影响^[7]. 刘彦菊等讨论了薄膜材料参数对其稳定性的影响^[8]. 不过目前大多数文献多分析准静态问题, 这方面的研究成果也较多. 但实际许多物理问题本质上是受周期载荷作用的动态问题, 因此对问题的动力响应进行分析就很必要. 目前动力响应问题的分析结果大多仅限于突加常值载荷的作用^[9], 对随时间变化的周期性载荷作用的结构动力响应的分析尚少见报道^[10-11]. 何新振等研究了电活性聚合

物圆柱壳在静态和周期电压作用下的响应及稳定性问题^[12].

本文的目的是根据有限变形动力学理论, 分析电活性聚合物圆柱壳在周期性载荷作用下的变形和破坏等大变形动力响应问题. 首先从基本方程得到了问题的控制方程组, 即描述圆柱壳内表面运动的二阶非线性常微分方程, 通过对变换后的一阶方程组进行 Runge-Kutta 积分法数值模拟, 得到了方程的解及振动的时程曲线、相图、庞加莱截面图等结果. 根据通常的动力学定性分析理论, 讨论了圆柱壳的动力响应特性, 各种条件下的破坏情况及电压的影响.

1 问题的数学描述

考虑一个内径为 A , 外径为 B , 长度为 L 的不可压电活性聚合物圆柱壳, 如图 1 所示, 在初始时刻 $t = 0$ 于内表面受到内压 $p(t) = p_1 + p_2 \sin \omega t$ 及在圆筒内外表面施加电压 Φ 作用下的大变形运动和破坏问题. 设圆柱壳变形后, 其内径为 a , 外径为 b , 长度为 l . 分别取物质坐标系和空间坐标系为 (R, Θ, Z) 和 (r, θ, z) , 则圆柱壳的运动模式为

$$r = r(R, t), \theta = \Theta, z = \lambda_z Z, (A \leq R \leq B) \quad (1)$$

式中, $r(R, t)$ 为待定函数, 轴向拉伸 λ_z 为圆柱壳预

2014-09-02 收到第 1 稿, 2015-05-26 收到修改稿.

* 上海市重点学科建设资助项目(S30106)

† 通讯作者 E-mail: renjiusheng@staff.shu.edu.cn

加应变限制,是一预先给定的常数.由材料的不可压条件

$$[r^2(R) - a^2]l = (R^2 - A^2)L$$

可得圆柱壳的变形函数

$$r = r(R, t) = \left[\frac{1}{\lambda_z} (R^2 - A^2) + a^2 \right]^{\frac{1}{2}} \quad (2)$$

式中, $a = r(R, t)$ 为变形后圆柱壳的内半径. 相应圆柱壳的主伸长.

$$\lambda_r = \frac{\partial r(R, t)}{\partial R} = \frac{R}{r\lambda_z}, \lambda_\theta = \frac{r(R, t)}{R} = \frac{r}{R}, \lambda_z = \frac{l}{L} \quad (3)$$

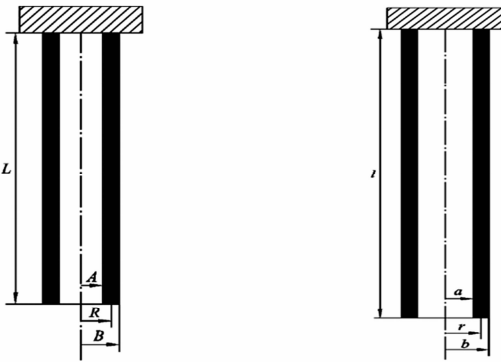


图1 圆柱壳的变形示意图

Fig. 1 The undeformed and deformed configurations of the cylindrical shell

这里考虑广义不可压 Ogden 电活性聚合物材料^[13]

$$W = \sum_{i=1}^3 \frac{\mu_i}{a_i} (\lambda_r^{a_i} + \lambda_\theta^{a_i} + \lambda_z^{a_i} - 3) + \frac{D^2}{2\varepsilon} \lambda_r \lambda_\theta \lambda_z \quad (4)$$

式中, ε 为材料的介电常数, 取 $\varepsilon = 2.21 \times 10^{-11}$ F/m^[14], D 为径向电位移, 材料常数值如下^[13]

$$\begin{aligned} \mu_1 &= 6.3 \times 10^5 \text{ Pa}, \mu_2 = 1.2 \times 10^3 \text{ Pa}, \\ \mu_3 &= -1 \times 10^4 \text{ Pa}, \\ a_1 &= 1.3, a_2 = 5, a_3 = -2, \end{aligned}$$

电活性聚合物的应力包括 Cauchy 应力和 Maxwell 应力两部分,

$$\begin{aligned} \sigma_{rr}(r, t) &= \sum_{i=1}^3 \mu_i \lambda_r^{a_i} - P(r, t) + \frac{D^2}{2\varepsilon} \\ \sigma_{\theta\theta}(r, t) &= \sum_{i=1}^3 \mu_i \lambda_\theta^{a_i} - P(r, t) - \frac{D^2}{2\varepsilon} \\ \sigma_{zz}(r, t) &= \sum_{i=1}^3 \mu_i \lambda_z^{a_i} - P(r, t) - \frac{D^2}{2\varepsilon} \end{aligned} \quad (5)$$

式中, $P(r, t)$ 为静水压力. 对圆柱壳而言, 电位移 D 和电势 Φ 与电量 Q 的关系分别为

$$\begin{aligned} D &= \frac{Q}{2\pi r \lambda_z L} \\ \Phi &= \frac{Q}{2\pi \varepsilon \lambda_z L} \log \frac{b}{a} \end{aligned} \quad (6)$$

于是

$$D = \frac{\Phi \varepsilon}{r \left(\log \frac{b}{a} \right)} \quad (7)$$

圆柱壳的运动方程为

$$\frac{d\sigma_{rr}}{dr} + \frac{1}{r} (\sigma_{rr} - \sigma_{\theta\theta}) = \rho r'' \quad (8)$$

圆柱壳受周期载荷作用的边界条件为

$$\sigma_{rr}(a, t) = -p(t) \quad (9a)$$

$$\sigma_{rr}(b, t) = 0 \quad (9b)$$

满足无约束自然状态的初始条件为

$$\begin{aligned} r(R, 0) &= R \\ r'(R, 0) &= 0 \end{aligned} \quad (10)$$

电压的边界条件为

$$\begin{aligned} \Phi(A) &= 0 \\ \Phi(B) &= \varphi \end{aligned} \quad (11)$$

2 问题的求解

由不可压条件(2)可得

$$r''(t) = \frac{1}{r} \left[\left(1 - \frac{a^2}{r^2} \right) (a')^2 + aa'' \right] \quad (12)$$

将应力分量(5)代入运动方程(8), 并利用(12)可得:

$$\begin{aligned} \frac{d}{dr} \left[\sum_{i=1}^3 \mu_i \lambda_r^{a_i} - P(r, t) + \frac{D^2}{2\varepsilon} \right] + \\ \frac{1}{r} \left[\sum_{i=1}^3 \mu_i (\lambda_r^{a_i} - \lambda_\theta^{a_i}) + \frac{D^2}{\varepsilon} \right] = \\ \frac{\rho}{r} \left[\left(1 - \frac{a^2}{r^2} \right) (a')^2 + aa'' \right] \end{aligned} \quad (13)$$

上式对 r 积分可得

$$\begin{aligned} \sum_{i=1}^3 \mu_i \lambda_r^{a_i} - P(r, t) + P(a, t) + \\ \frac{\Phi^2 \varepsilon}{2r^2 \left(\log \frac{b}{a} \right)^2} + \int_a^r \sum_{i=1}^3 \mu_i (\lambda_r^{a_i} - \lambda_\theta^{a_i}) \frac{ds}{s} = \\ \rho [(a')^2 + aa''] (\ln r - \ln a) + \\ \frac{1}{2} \left[\rho a^2 (a')^2 + \frac{\Phi^2 \varepsilon}{\left(\log \frac{b}{a} \right)^2} \right] \left(\frac{1}{r^2} - \frac{1}{a^2} \right) \end{aligned} \quad (14)$$

将上式代入(9a)式可得:

$$\begin{aligned} \sigma_{rr}(r,t) = & \rho[(a')^2 + aa''](\ln r - \ln a) + \\ & \frac{1}{2}[\rho a^2(a')^2 + \frac{\Phi^2 \varepsilon}{(\log \frac{b}{a})^2}]\left(\frac{1}{r^2} - \frac{1}{a^2}\right) - \\ & \int_a^r \sum_{i=1}^3 \mu_i (\lambda_r^{a_i} - \lambda_\theta^{a_i}) \frac{ds}{s} - P(a,t) \end{aligned} \quad (15)$$

将式(15)代入边界条件(9a)可得

$$\sigma_{rr}(a,t) = -P(a,t) = -p(t)$$

即

$$P(a,t) = p(t)$$

将式(15)代入边界条件(9b)可得

$$\begin{aligned} p(t) = & \rho[(a')^2 + aa''](\ln b - \ln a) + \\ & \frac{1}{2}[\rho a^2(a')^2 + \frac{\Phi^2 \varepsilon}{(\log \frac{b}{a})^2}]\left(\frac{1}{b^2} - \frac{1}{a^2}\right) - \\ & \int_a^b \sum_{i=1}^3 \mu_i (\lambda_r^{a_i} - \lambda_\theta^{a_i}) \frac{dr}{r} \end{aligned} \quad (16)$$

引入变换

$$\frac{a}{A} = x(t),$$

$$\frac{B^2}{A^2} - 1 = \delta$$

则有

$$\begin{aligned} \frac{da(t)}{dt} = & A \frac{dx}{dt}, \quad \frac{d^2 a(t)}{dt^2} = A \frac{d^2 x}{dt^2} \\ \frac{b^2}{A^2} = & x^2(t) + \frac{\delta}{\lambda_z}, \quad \frac{b^2}{B^2} = \frac{x^2(t) + \delta/\lambda_z}{\delta + 1}, \\ \frac{b}{a} = & \sqrt{1 + \frac{\delta}{\lambda_z x^2}} \end{aligned}$$

令 $\xi = r/R$, 可得

$$\xi = \left[\lambda_z \left(1 - \frac{a^2}{r^2} \right) + \frac{A^2}{r^2} \right]^{-1/2}$$

$$\frac{dr}{r} = \frac{1}{1 - \lambda_z \xi^2} \frac{d\xi}{\xi}$$

于是式(16)可改写

$$\begin{aligned} p(t) = & \rho A^2 (x')^2 \left[\frac{-\delta}{2(\lambda_z x^2 + \delta)} + \ln \sqrt{1 + \frac{\delta}{\lambda_z x^2}} \right] + \\ & \rho A^2 x x'' \ln \sqrt{1 + \frac{\delta}{\lambda_z x^2}} + \\ & \frac{\Phi^2 \varepsilon}{2A^2 [\log \sqrt{1 + \delta/(\lambda_z x^2)}]^2} \left(\frac{1}{x^2 + \delta/\lambda_z} - \frac{1}{x^2} \right) - \\ & \int_x^{\sqrt{(x^2 + \delta/\lambda_z)/(\delta+1)}} \sum_{i=1}^3 \mu_i (\lambda_z^{-a_i} \xi^{-a_i} - \xi^{a_i}) \frac{d\xi}{\xi(1 - \lambda_z \xi^2)} \end{aligned} \quad (17)$$

其中 $a = xA, b = \sqrt{x^2 + \frac{\delta}{\lambda_z}} A$

相应的初始条件为

$$x(0) = 1, x'(0) = 0 \quad (18)$$

现引入变换

$$x_1 = x, x_2 = x'$$

则二阶微分方程(17)可改写

$$\begin{aligned} x_1' = & x_2, \\ x_2' = & \frac{x_2^2}{x_1 \ln \sqrt{1 + \delta/(\lambda_z x_1^2)}} \left[\frac{\delta}{2(\lambda_z x_1^2 + \delta)} - \right. \\ & \left. \ln \sqrt{1 + \frac{\delta}{\lambda_z x_1^2}} \right] + \frac{1}{\rho A^2 x_1 \ln \sqrt{1 + \delta/(\lambda_z x_1^2)}} \cdot \\ & \left\{ p(t) + \int_{x_1}^{\sqrt{(x_1^2 + \delta/\lambda_z)/(\delta+1)}} \sum_{i=1}^3 \mu_i (\lambda_z^{-a_i} \xi^{-a_i} - \xi^{a_i}) \frac{d\xi}{\xi(1 - \lambda_z \xi^2)} - \right. \\ & \left. \frac{\Phi^2 \varepsilon}{2A^2 [\log \sqrt{1 + \delta/(\lambda_z x_1^2)}]^2} \left(\frac{1}{x_1^2 + \delta/\lambda_z} - \frac{1}{x_1^2} \right) \right\} \end{aligned} \quad (19)$$

相应的初始条件为

$$x_1(0) = 1, x_2(0) = 0 \quad (20)$$

3 结果与讨论

对圆柱壳在形如 $p(t) = p_1 + p_2 \sin \omega t$ 的周期载荷作用下的动力响应和破坏, 利用 Runge-Kutta 方法对微分方程组(19)和初始条件(20)进行数值计算可得到圆柱壳变形的时程曲线、相图和庞加莱截面图等结果. 这里我们取周期载荷为 $p(t) = p_1 + p_2 \sin 2\pi t$, 所得图形如下: 时程曲线如图 2~5 所示, 相图及庞加莱截面图如图 6~9 所示.

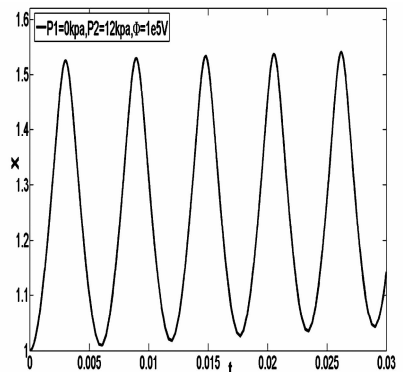


图2 时程曲线 $P_1 = 0, P_2 = 12\text{kPa}, \Phi = 1 \times 10^5 \text{V}$

Fig. 2 Time history responses, $P_1 = 0, P_2 = 12\text{kPa}, \Phi = 1 \times 10^5 \text{V}$

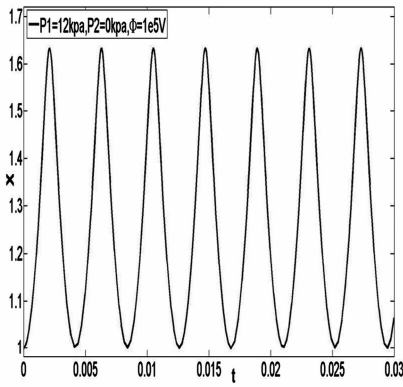


图3 时程曲线 $P_1 = 12\text{Kpa}, P_2 = 0, \Phi = 1 \times 10^5 \text{V}$

Fig. 3 Time history responses,
 $P_1 = 12\text{Kpa}, P_2 = 0, \Phi = 1 \times 10^5 \text{V}$

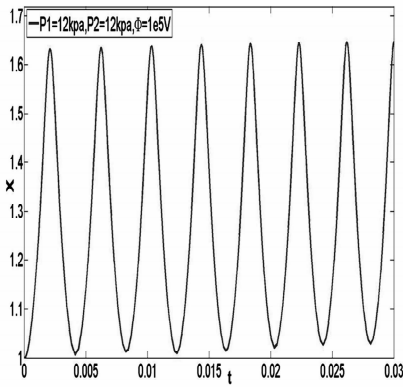


图4 时程曲线 $P_1 = 12\text{Kpa}, P_2 = 12\text{Kpa}, \Phi = 1 \times 10^5 \text{V}$

Fig. 4 Time history responses,
 $P_1 = 12\text{Kpa}, P_2 = 12\text{Kpa}, \Phi = 1 \times 10^5 \text{V}$

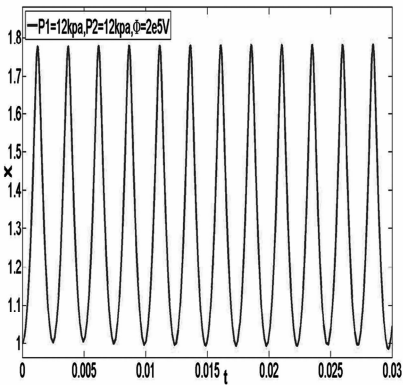


图5 时程曲线 $P_1 = 12\text{Kpa}, P_2 = 12\text{Kpa}, \Phi = 2 \times 10^5 \text{V}$

Fig. 5 Time history responses,
 $P_1 = 12\text{Kpa}, P_2 = 12\text{Kpa}, \Phi = 2 \times 10^5 \text{V}$

由图可见,圆柱壳的时程曲线不是典型的周期运动曲线,相图由几个封闭的曲线组成,庞加莱截面图由不规则分布的点组成.

对周期载荷 $p(t) = p_1 + p_2 \sin 2\pi t$ 而言,其平均

载荷为 $p_m = p_1 + p_2$. 计算过程表明,对给定的幅值载荷 p_2 和载荷频率 ω 及外加电压 Φ ,平均载荷存在一个临界值 p_{cr} . 当 $p_m < p_{cr}$ 时,图2~图9给出的时程曲线、相图及庞加莱截面图结果可通过数值计算得到,且图2~图9各图表明在周期载荷作用下圆柱壳的运动为拟周期性的非线性振动. 但当 $p_m \geq p_{cr}$ 时,不能得到图2~图9各图,意味着圆柱壳将被载荷破坏^[12].

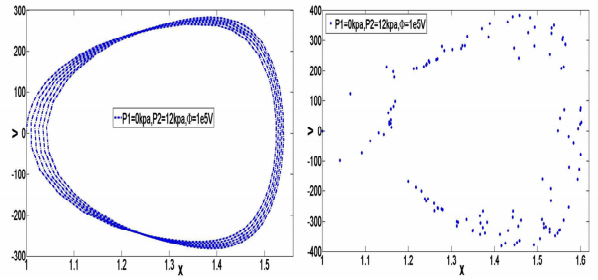


图6 相图及其庞加莱截面图

$\delta = 0.11, P_1 = 0, P_2 = 12\text{Kpa}, \Phi = 1 \times 10^5 \text{V}, \omega = 2\pi$

Fig. 6 Phase portrait and Poincaré map,

$\delta = 0.11, P_1 = 0, P_2 = 12\text{Kpa}, \Phi = 1 \times 10^5 \text{V}, \omega = 2\pi$

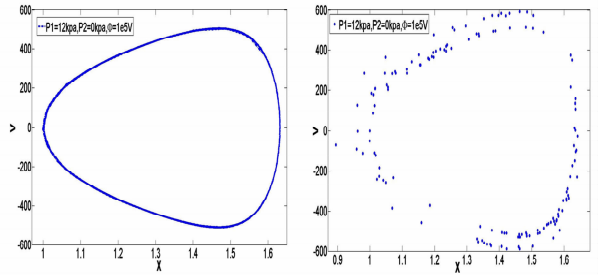


图7 相图及其庞加莱截面图

$\delta = 0.11, P_1 = 12\text{Kpa}, P_2 = 0, \Phi = 1 \times 10^5 \text{V}, \omega = 2\pi$

Fig. 7 Phase portrait and Poincaré map,

$\delta = 0.11, P_1 = 12\text{Kpa}, P_2 = 0, \Phi = 1 \times 10^5 \text{V}, \omega = 2\pi$

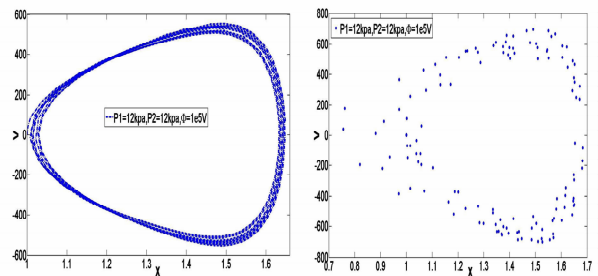


图8 相图及其庞加莱截面图

$\delta = 0.11, P_1 = 12\text{Kpa}, P_2 = 12\text{Kpa}, \Phi = 1 \times 10^5 \text{V}, \omega = 2\pi$

Fig. 8 Phase portrait and Poincaré map,

$\delta = 0.11, P_1 = 12\text{Kpa}, P_2 = 12\text{Kpa}, \Phi = 1 \times 10^5 \text{V}, \omega = 2\pi$

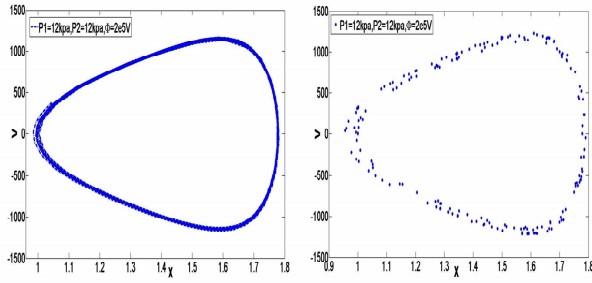


图9 相图及其庞加莱截面图

$$\delta = 0.11, P_1 = 12\text{Kpa}, P_2 = 12\text{Kpa}, \Phi = 2 \times 10^5 \text{V}, \omega = 2\pi$$

Fig. 9 Phase portrait and Poincaré map ,

$$\delta = 0.11, P_1 = 12\text{Kpa}, P_2 = 12\text{Kpa}, \Phi = 2 \times 10^5 \text{V}, \omega = 2\pi$$

同时外加电压也存在一个临界值 Φ_{cr} 。当 $\Phi < \Phi_{cr}$ ，在周期载荷作用下，圆柱壳的运动为拟周期性的非线性振动。对比图4，图5发现，当圆柱壳的运动为拟周期性的非线性振动时，电压增加时，振幅增大，振动周期减小，同时拟周期运动的不规则程度变得更严重。结果表明外加电压会加剧圆柱壳的振动，减小圆柱壳的振动周期。当 $\Phi \geq \Phi_{cr}$ 时不能得到图2~图9各图，圆柱壳将被破坏^[12]。

总之，当 $p_m < p_{cr}$ 且 $\Phi < \Phi_{cr}$ 时，在周期载荷作用下圆柱壳的运动为拟周期性的非线性振动。且此时平均载荷值 p_m 越大，拟周期运动的不规则程度越严重。外加电压 Φ 越大，拟周期运动的不规则程度也越严重。

另外，计算结果表明，载荷幅值 p_1 对圆柱壳的拟周期性振动有较大影响，载荷幅值 p_2 对圆柱壳的拟周期性振动的影响可忽略不计。对比图2~4发现， p_1 越大，拟周期振动的振幅越大，振动周期越短，拟周期运动的不规则程度越严重。载荷幅值 p_2 和载荷频率 ω 对临界载荷值 p_{cr} 的影响可忽略不计，如对 $\delta = 0.11$ 的圆柱壳，其临界载荷值 p_{cr} 几乎总为 63Kpa。

图10为 $\omega = 64\pi$ 时的时程曲线和相图，与 $\omega = 2\pi$ 的时程曲线和相图结果相比发现，频率越大，振动周期无明显变化，振幅略有增加，但拟周期运动的不规则程度越严重。

4 结论

本文基于有限变形动力学理论，分析了不可压电活性聚合物圆柱壳在周期载荷作用下的动力响应和破坏问题。发现对周期载荷存在着其平均载荷

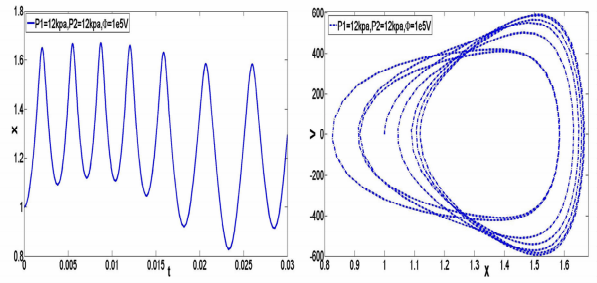


图10 时程曲线和相图

$$\delta = 0.11, P_1 = 12\text{Kpa}, P_2 = 12\text{Kpa}, \Phi = 1 \times 10^5 \text{V}, \omega = 64\pi$$

Fig. 10 Time history responses and Phase portrait ,

$$\delta = 0.11, P_1 = 12\text{Kpa}, P_2 = 12\text{Kpa}, \Phi = 1 \times 10^5 \text{V}, \omega = 64\pi$$

的一个临界值，当平均载荷小于这个临界值时，时程曲线、相图及庞加莱截面图可通过数值计算得到，圆柱壳的运动为拟周期性的非线性振动。但当平均载荷大于这个临界值时，不能得到以上各图，圆柱壳将被破坏。外加电压也存在一个临界值。当外加电压小于这个临界值时，在周期载荷作用下，圆柱壳的运动为拟周期性的非线性振动。当圆柱壳的运动为拟周期性的非线性振动时，电压增加时，振幅增大，振动周期缩短，同时拟周期运动的不规则程度变得更严重。表明电压会加剧圆柱壳的振动，减小圆柱壳的振动周期。当外加电压大于这个临界值时，圆柱壳将被破坏。

参 考 文 献

- 1 Kim K J, Tadoro S. *Electroactive Polymers for Robotic Applications*. London: Springer, 2007
- 2 Gallone G, Carpi F, Rossi D D, Levita G, Marchetti A. Dielectric constant enhancement in a silicone elastomer filled with lead magnesium niobate-lead titanate. *Materials Science and Engineering: C*, 2007, 27(1): 110 ~ 116
- 3 Aschwanden M, Beck M, Stemmer A. Diffractive transmission grating tuned by dielectric elastomer actuator. *IEEE Photonics Technology Letters*, 2007, 19(14): 1090 ~ 1092
- 4 Pelrine R, Kornbluh R, Pei Q, et al. High-speed electrically actuated elastomers with strain greater than 100%. *Science*, 2000, 287: 836 ~ 839
- 5 Suo Z G, Zhao X H, Greene W H. A nonlinear field theory of deformable dielectrics. *Journal of the Mechanics and Physics of Solids*, 2008, 56(2): 467 ~ 486
- 6 He T H, Zhao X H, Suo Z G. Dielectric elastomer membranes undergoing inhomogeneous deformation. *Journal of*

- Applied Physics*, 2009, 106(8): 083522 ~ 083529
- 7 Plante J, Dubowsky S. Large-scale failure modes dielectric elastomer actuators. *International Journal of Solids and Structures*, 2006, 43(25-26): 7727 ~ 7751
- 8 刘彦菊, 孙寿华, 刘立武等. 具有线性介电常数的 Ogden 型介电弹性体的本构关系和机电稳定性. 固体力学学报, 2010, 31(2): 181 ~ 192 (Liu L W, Sun S H, Liu Y J, et al. Constitutive relation electromechanical stability analysis of Ogden type dielectric elastomer with linear permittivity. *Chinese Journal of Solid Mechanics*, 2010, 31(2): 181 ~ 192 (in Chinese))
- 9 Calderer C. The dynamical behavior of nonlinear elastic spherical shells. *Journal of Elasticity*, 1983, 13(1): 17 ~ 47
- 10 田磊, 吴莹, 王铁军. 阻尼对泡沫夹芯梁非线性振动响应的影响. 动力学与控制学报, 2013, 11(1): 53 ~ 57 (Tian L, Wu Y, Wang T J. Effect of damping on nonlinear vibration of metal foam sandwich beam. *Journal of Dynamics and Control*, 2013, 11(1): 55 ~ 57 (in Chinese))
- 11 任九生. 热超弹性圆柱壳的振动与破坏. 振动与冲击, 2008, 27(12): 36 ~ 39 (Ren J S. Vibration and damage of hyper-Elastic cylindrical shells under heat. *Journal of Vibration and Shock*, 2008, 27(12): 36 ~ 39 (in Chinese))
- 12 何新振, 雍华东, 周又和. 电活性聚合物圆柱壳静态与动态电压下的响应及稳定性. 固体力学学报, 2012, 33(4): 341 ~ 347 (He X Z, Yong H D, Zhou Y H. The response and stability of electro-active polymer cylindrical shells under the static and dynamic voltage. *Chinese Journal of Solid Mechanics*, 2012, 33(4): 341 ~ 347 (in Chinese))
- 13 Stephan R, Kaushik B, deBotton G. Snap-through actuation of thick-wall electroactive balloons. *International Journal of Non-Linear Mechanics*, 2012, 47: 206 ~ 209
- 14 Díaz-Calleja R, Riande E, Sanchis M J. On electromechanical stability of dielectric elastomers. *Applied Physics Letters*, 2008, 93(10): 101902

DYNAMICAL RESPONSE OF ELECTRO-ACTIVE POLYMER CYLINDRICAL SHELLS UNDER PERIODIC PRESSURE*

Wang Chengmin¹ Ren Jiusheng²

(1. Shanghai Institute of Applied Mathematics and Mechanics, Shanghai 200072, China)

(2. Department of Mechanics, Shanghai Key Laboratory of Mechanics in Energy and Environment Engineering, Shanghai University, Shanghai 200444, China)

Abstract The dynamical response including the motion and the destruction of the electro-active polymer cylindrical shells subjected to the periodic pressure on the inner surface are studied within the framework of finite elasto-dynamics. It is proved that there exists a certain critical value of the internal pressure and the electric field through numerical computing and dynamic qualitative analysis based on the nonlinear differential equation for the motion of the inner surface of the shell. The motion of the shell is nonlinear quasi-periodic oscillation when the mean pressure of the periodic pressure and the voltage are less than their critical values, respectively. In contrast, the shell is destroyed when the pressure or the voltage exceeds the corresponding critical value. Moreover, the effect of the electric field and the pressure parameters on the critical values and the oscillation of the shell are then discussed.

Key words electro-active polymer, nonlinear differential equation, quasi-periodic oscillation, critical pressure, destruction